


RESEARCH ARTICLE

Open Access



# Single-cell peripheral immunoprofiling of lewy body and Parkinson's disease in a multi-site cohort

Thanaphong Phongpreecha<sup>1,2,3</sup> , Kavita Mathi<sup>4</sup>, Brenna Cholerton<sup>1</sup>, Eddie J. Fox<sup>1</sup>, Natalia Sigal<sup>4</sup>, Camilo Espinosa<sup>2,3,5</sup>, Momsen Reincke<sup>2,3,5</sup>, Philip Chung<sup>2</sup>, Ling-Jen Hwang<sup>3</sup>, Chandresh R. Gajera<sup>1</sup>, Eloise Berson<sup>1,2,3</sup>, Amalia Perna<sup>1</sup>, Feng Xie<sup>2,3,5</sup>, Chi-Hung Shu<sup>2,3,5</sup>, Debapriya Hazra<sup>2,3,5</sup>, Divya Channappa<sup>6</sup>, Jeffrey E. Dunn<sup>6</sup>, Lucas B. Kipp<sup>6</sup>, Kathleen L. Poston<sup>6</sup>, Kathleen S. Montine<sup>1</sup>, Holden T. Maecker<sup>4</sup>, Nima Aghaepour<sup>2,3,5</sup> and Thomas J. Montine<sup>1\*</sup>

## Abstract

**Background** Multiple lines of evidence support peripheral organs in the initiation or progression of Lewy body disease (LBD), a spectrum of neurodegenerative diagnoses that include Parkinson's Disease (PD) without or with dementia (PDD) and dementia with Lewy bodies (DLB). However, the potential contribution of the peripheral immune response to LBD remains unclear. This study aims to characterize peripheral immune responses unique to participants with LBD at single-cell resolution to highlight potential biomarkers and increase mechanistic understanding of LBD pathogenesis in humans.

**Methods** In a case-control study, peripheral mononuclear cell (PBMC) samples from research participants were randomly sampled from multiple sites across the United States. The diagnosis groups comprise healthy controls (HC, n = 159), LBD (n = 110), Alzheimer's disease dementia (ADD, n = 97), other neurodegenerative disease controls (NDC, n = 19), and immune disease controls (IDC, n = 14). PBMCs were activated with three stimulants (LPS, IL-6, and IFN $\alpha$ ) or remained at basal state, stained by 13 surface markers and 7 intracellular signal markers, and analyzed by flow cytometry, which generated 1,184 immune features after gating.

**Results** The model classified LBD from HC with an AUROC of  $0.87 \pm 0.06$  and AUPRC of  $0.80 \pm 0.06$ . Without retraining, the same model was able to distinguish LBD from ADD, NDC, and IDC. Model predictions were driven by pPLC $\gamma$ 2, p38, and pSTAT5 signals from specific cell populations under specific activation. The immune responses characteristic for LBD were not associated with other common medical conditions related to the risk of LBD or dementia, such as sleep disorders, hypertension, or diabetes.

**Conclusions and Relevance** Quantification of PBMC immune response from multisite research participants yielded a unique pattern for LBD compared to HC, multiple related neurodegenerative diseases, and autoimmune diseases thereby highlighting potential biomarkers and mechanisms of disease.

**Keywords** Parkinson's Disease, Alzheimer's Disease, Biomarkers, Dementia, Inflammation

\*Correspondence:  
Thomas J. Montine  
tmontine@stanford.edu  
Full list of author information is available at the end of the article



## Background

Lewy Body Disease (LBD) comprises a spectrum of clinically and pathologically overlapping conditions: Dementia with Lewy Bodies (DLB) and Parkinson's Disease (PD) with or without Dementia (PDD) [1–5]. Human genetic, biochemical, and pathological evidence, as well as experimental models, support involvement not only by neuroinflammation [6–8] but also a peripheral immune response in the initiation and/or progression of LBD [6, 9–13]. While there is intense interest in the systemic origins of pathologic alpha-synuclein, the role of the peripheral immune system in LBD remains unclear. One possibility is that subsets of peripheral immune cells migrate into the brain and consequently play a direct role in neurodegeneration [14]. Alternatively, peripheral immune cells may serve as biomarkers of an inherited or acquired trait shared by both peripheral and brain immune cells without peripheral cells directly contributing to neurodegeneration. Past research has explored peripheral blood mononuclear cells (PBMCs) as a platform to gain insights into the development of LBD with a focus on changes in the proportion of specific cell types [15–20] or concentration of intercellular signals such as interleukins (ILs) [21–24]. While alteration of intracellular signaling in PBMCs of cognitively impaired or Alzheimer's Disease (AD) participants has been explored previously [25–29], only a handful of studies have profiled PBMC intracellular signaling for LBD [30–32]. Moreover, most of these investigations of PBMCs in LBD have been limited by small sample sizes, single cohorts, bulk analysis, and lack of disease controls to determine non-specific changes related to neurodegenerative diseases or immune-mediated diseases.

This study sought to address several of these limitations through a rigorous profiling of peripheral immune responses by PBMCs from 399 age- and sex-matched multisite research participants diagnosed with LBD, other neurodegenerative diseases (NDC), or healthy controls (HC). Fourteen additional samples also were obtained from participants at a single site who were diagnosed with autoimmune disease. Samples were unstimulated or activated with three different canonical immune stimulants to gain functional insight and then assayed with a panel of markers that resolved 37 different cell types and the intracellular signaling pathways that were selected to encompass those previously implicated by genetic risk and their associated pathways [33–36]. Specifically, the cytometry panel and stimulants were selected such that the surface markers allow us to maximize the number of different immune cell types and to cover the cell types with strong signals for neurodegenerative diseases from our prior work [25]. The intracellular signals were a subset of our previous study and were

chosen due to their relatedness to neurodegenerative diseases through different proposed mechanisms. For example, *PLCG2* was previously suggested to have a broad influence on the mechanisms of microglial activity and preserving synaptic integrity related to neurodegeneration [37–40], peripheral pSTATs were indicated for AD in our previous study [25], and p38 MAPK was involved in the process of neuronal death in various neurodegenerations [41, 42].

## Methods

### Study design

This study aimed to determine whether differences in peripheral immune responses between healthy controls (HC) and research participants with LBD (PD, PDD, and DLB) are detectable by flow cytometry analysis of PBMCs. In addition, we included samples from other research participants for neurodegenerative disease controls (NDC) and participants with autoimmune diseases for immune disease controls (IDC) to control for nonspecific effects of debilitation from neurodegeneration and immune-mediated diseases, neither group was used to train the model in any part, but to evaluate for nonspecific effects that debilitation from neurodegeneration might have on the PBMC response to stimulation. Diagnoses (ADD, PD, LBD, NDCs) were made using published diagnostic criteria, as described in the NACC Uniform Data Set Coding Guidebook (Version 3, 2015) [43–48] and multiple sclerosis (MS) diagnosis in IDC group were made using the 2017 McDonald criteria [49]. Participants were research volunteers at Stanford Alzheimer's Disease Research Center or the Pacific Udall Center (Stanford ADRC), Stanford BIG Project (BIG), and many other Alzheimer's Disease Research Centers (ADRCs), whose samples were aggregated and distributed by the National Centralized Repository for Alzheimer's Disease and Related Dementias (NCRAD). All participants provided written informed consent to participate in the study, which followed protocols approved by the Stanford Institutional Review Board. Clinical diagnosis was made by consensus criteria.

Blood was collected from a total of 399 volunteers stratified into seven diagnosis groups: HC ( $n=159$ ), LBD (total  $n=110$  including 60 PD without dementia, 32 PD with dementia (PDD), and 18 DLB), Alzheimer's disease dementia (ADD,  $n=97$ ), other neurodegenerative disease controls (NDC;  $n=19$ ), and immune disease controls (IDC;  $n=14$ ). Diseases comprising NDC were frontotemporal lobar degeneration ( $n=6$ ), primary progressive aphasia ( $n=2$ ), vascular brain injury ( $n=8$ ), and traumatic brain injury ( $n=3$ ). IDC group were participants with primary ( $n=8$ ) and secondary ( $n=6$ ) progressive multiple sclerosis. HCs were individuals who were

not diagnosed with any neurological disease and had no cognitive impairment. AD, LBD (PD/PDD/DLB), and NDC participants had a single clinical diagnosis without clinical comorbidity. Demographic data for each group is shown in Table 1. The percent contribution of each diagnosis group from each site was 35% Stanford ADRC and 65% NCRAD for HC, 35% Stanford ADRC and 65% NCRAD for ADD, 92% Stanford ADRC and 8% NCRAD for LBD, 100% NCRAD for NDC, 100% BIG for IDC. Beyond diagnoses, the associated data include information collected by NACC, such as demographics, cognitive exam scores, Unified Parkinson's Disease Rating Scale (UPDRS), and non-neurodegenerative disease comorbidities. However, this study did not have data on the presence of fever and/or recent infectious processes, and hence their effects were not assessed. The protocol for PBMC collection and storage by each site can be found in the Supplementary Materials.

#### Flow cytometry experiment

All cytometry experiments were performed at Stanford. Samples from different diagnosis groups were randomly

and blindly assigned to each of the 42 batches to prevent confounding between diagnoses and batches. PBMCs were isolated by density-gradient centrifugation and cryopreserved. Post-thaw, cells were washed in a complete RPMI medium with benzonase. Cell viability as measured by Vi-Cell (Beckman Coulter) for all samples was above 90%. After resting for 2 h at 37 °C, PBMCs were either left unstimulated or stimulated with one of three stimulants: IFN $\alpha$  (10,000 units/ml), IL-6 (50 ng/ml) or LPS (200 ng/ml) for 15 min, at 37 °C. Stimulation was stopped by fixing cells with paraformaldehyde for 10 min at room temperature. Stimulant doses and exposure time points were optimized in our previous studies [50]. PBMCs from healthy donors at the Stanford Blood Center, whose phosphoprotein responses to stimulation were well-characterized in our lab, were used for quality assurance. Including these positive control samples with each batch ensured the expected phosphorylation response from the controls and validated the stimulation and staining conditions [50–52]. After washing cells with PBS, samples were stained with LIVE/DEAD™ Fixable Blue Dead Cell Stain Kit, for UV excitation (from Invitrogen) for 15 min

**Table 1** Cohort statistic summary stratified by diagnosis groups

	HC n = 159	AD n = 97	LBD n = 110	NDC n = 19	IDC n = 14	Overall P* Pairwise
<b>Age</b>						
Mean (SD)	73.0 (6.0)	74.8 (8.0)	72.2 (7.2) 52-	73.4 (6.9)	67.2 (3.3) 63	0.002
Range	55–95	51–91	92	67–84	- 74	AD, HC > IDC
<b>Gender</b>						
N (%) Female	90 (56.6%)	57 (58.8%)	50 (45.5%)	12 (63.2%)	10 (71.4%)	0.147
<b>Race N (%)</b>						
White	126 (80.8%)	84 (88.4%)	99 (94.3%)	16 (84.2%)	13 (92.9%)	0.123
Black	2 (1.3%)	1 (1.1%)	-	-	1 (7.1%)	
American Indian/Alaskan Native	1 (0.6%)	-	1 (1.0%)	-	-	
Native Hawaiian/Pacific Islander	-	-	-	-	-	
Asian	25 (16.0%)	9 (9.5%)	5 (4.8%)	-	-	
Other/mixed race	2 (1.3%)	1 (1.1%)	-	3 (15.8%)	-	
<b>Education</b>						
Mean (SD)	16.9 (2.3)	15.8 (3.2)	17.1 (2.3)	16.4 (3.5)	-	0.003
Range	12–22	8–24	12–20	8–23	-	LBD, HC > AD
<b>Cognitive status N (%)</b>						
No cognitive impairment	162 (100.0%)	-	55 (53.4%)	9 (47.4%)	-	LBD vs. NDC:
CIND	-	-	30 (29.1%) 18 (17.5%)	4 (21.1%)	-	0.399
Dementia	-	96 (100.0%)	-	6 (31.6%)	-	
<b>Use of AD medications</b>						
N (%)	-	64 (66.0%)	20 (19.1%)	3 (15.8%)	-	< 0.0001 AD > LBD, NDC
<b>Use of PD medications</b>						
N (%)	-	3 (4.8%)	80 (87.9%)	3 (15.8%)	-	< 0.0001 LBD > AD, NDC

**Abbreviations:** AD Alzheimer' disease, CIND Cognitively impaired, but not dementia, HC healthy controls, IDC immune disease controls, LBD Lewy body disease, NDC neurodegenerative disease controls, PD Parkinson's disease

\* P values based on one way ANOVA for continuous variables and chi-square or Fisher's exact tests for categorical variables

at room temperature. After live dead staining, cells were washed with wash buffer (Phosphate buffered saline, 2% Fetal bovine serum, 0.1% sodium azide), followed by surface staining with anti- CD4(BUV805), CD7 (AF780), CD8 (AF700), CD11b (BUV395), CD14 (BUV737), CD16 (BV750), CD19 (PerCP-Cy5.5), CD27 (BV711), CD56 (BUV563), CD69 (BUV661), HLA-DR (BV480) (antibodies from BD Biosciences), CD3 (BV605) and CD45RA (BV570) (antibodies from BioLegend). Staining was done at room temperature for 30 min. After 2 washes, cells were permeabilized with ice-cold methanol and were stored overnight at -80 °C. Post permeabilization, cells were washed again, and intracellular staining was done with anti-pSTAT1 (AF488), pSTAT5 (PE-Cy7), pP38 (PE), pPLC $\gamma$ 2 (APC), pS6 (BV421), CD107b/Lamp2 (BV786), (antibodies from BD Biosciences) and Rab5 (PE-CF594) (from Santa Cruz Biotechnology) at room temperature for 30 min. After two further washes, the acquisition was performed on a BD Symphony A5 flow cytometer with a High Throughput Sampler (HTS) and analyzed using FlowJo software where median expressions were collected for each gated cell type. The reagents and the gating scheme can be found in Table S1 and Fig. S1. To mitigate possible confounded effects between class imbalance between sites, the Combat algorithm by the pyCombat [53] package was used. Combat removes site effects by modeling the data as a combination of site effects and biological signals, then use empirical Bayes to estimate the site effect parameters and subtract them, normalizing the data across batches while retaining the true biological variation [54]. Note that there was no missing data from flow cytometry and no outliers were excluded. Eight participants were excluded due to ambiguous diagnoses: five HCs who took PD medications, an HC who in later visits showed cognitive impairment, an AD participant with an unclear AD diagnosis, and an NDC with a NACC etiologic diagnosis of "Other."

#### Data analysis

Machine learning is a common tool for extracting insight from high-dimensional cytometry data [55, 56]. Here, light gradient-boosting machine (LGBM) [57] was used as it outperformed other machine learning models (Fig. S2), including logistic linear, random forest, and feed-forward neural network models, in our dataset. To maximize generalizability, the performance was evaluated using 10 repeated fourfold cross-validation. In each iteration, the data were randomly split into 4 equal portions. The model was trained on 3 of those (training set), and tested/evaluated on the last unseen portion (test set). Due to the random nature, the train/test samples in each iteration were different. This provided a comprehensive view of the model's performance. For the classification

of the three main groups, HC and IDC were merged and labeled 0, and the disease group (LBD or ADD) was labeled 1. The test set prediction values were used for subsequent analyses and visualizations. The model performance metrics include the Area Under the Receiving Operating Characteristic (AUROC) and the Area Under the Precision-Recall Curve (AUPRC). For differential predictions, *e.g.* ADD vs. LBD or NDC vs. LBD, the primary model trained for HC vs. LBD was used without retraining. For the prediction of LBD subgroups (PD, PDD, DLB), comorbidities, and motor examinations, LGBM was also used with the same cross-validation setup except that a subsampling technique was used to ensure balanced age and sex ratios between case and controls. Methods for model reduction and correlation networks can be found in the Supplementary Materials.

## Results

### Overview of the cohort and immune features

Samples were from individuals with one of these clinical diagnoses: healthy controls (HC), LBD, ADD, other neurodegenerative disease controls (NDC), or autoimmune disease controls (IDC) (Table 1). All diagnosis groups were exclusive, *e.g.* no participants were diagnosed with both LBD and AD. Each individual's PBMCs were stimulated with LPS, IFN $\alpha$ , IL6, or unstimulated, followed by staining and measurement of cell type-specific abundance and intracellular signaling (see Methods Section), including Lamp2, p38, pPLC $\gamma$ 2, pS6, pSTAT1, pSTAT5, and Rab5. After cell type gating, there were 1,184 immune features total in each of the 399 individual PBMC samples (Fig. 1A).

The immune feature landscape (Fig. 1B) indicates that, regardless of stimulation and cell type, features from the same intracellular signals tended to be highly correlated with each other, aligning with known intracellular signaling cascades. A subset of pSTAT1, pSTAT5, and pPLC $\gamma$ 2 were highly correlated, whereas pS6 was the least correlated to other signals. A t-SNE plot for participants landscape colored by site indicated that batch correction was effective as there was no apparent site-specific cluster (Fig. 1C left). While there could be other confounding factors other than sites, Fig. 1C shows that all diagnosis groups were well distributed, hence allaying concerns of any strong effects introduced by confounders.

### Immune features differentiate LBD from HC and other diseases

The machine learning model (LGBM) exhibited strong performance for separating LBD from HC (Area Under the Receiver Operating Curve [AUROC]=0.87 $\pm$ 0.06, Area Under Precision-Recall Curve [AUPRC]=0.80 $\pm$ 0.06; the AUROC corresponds

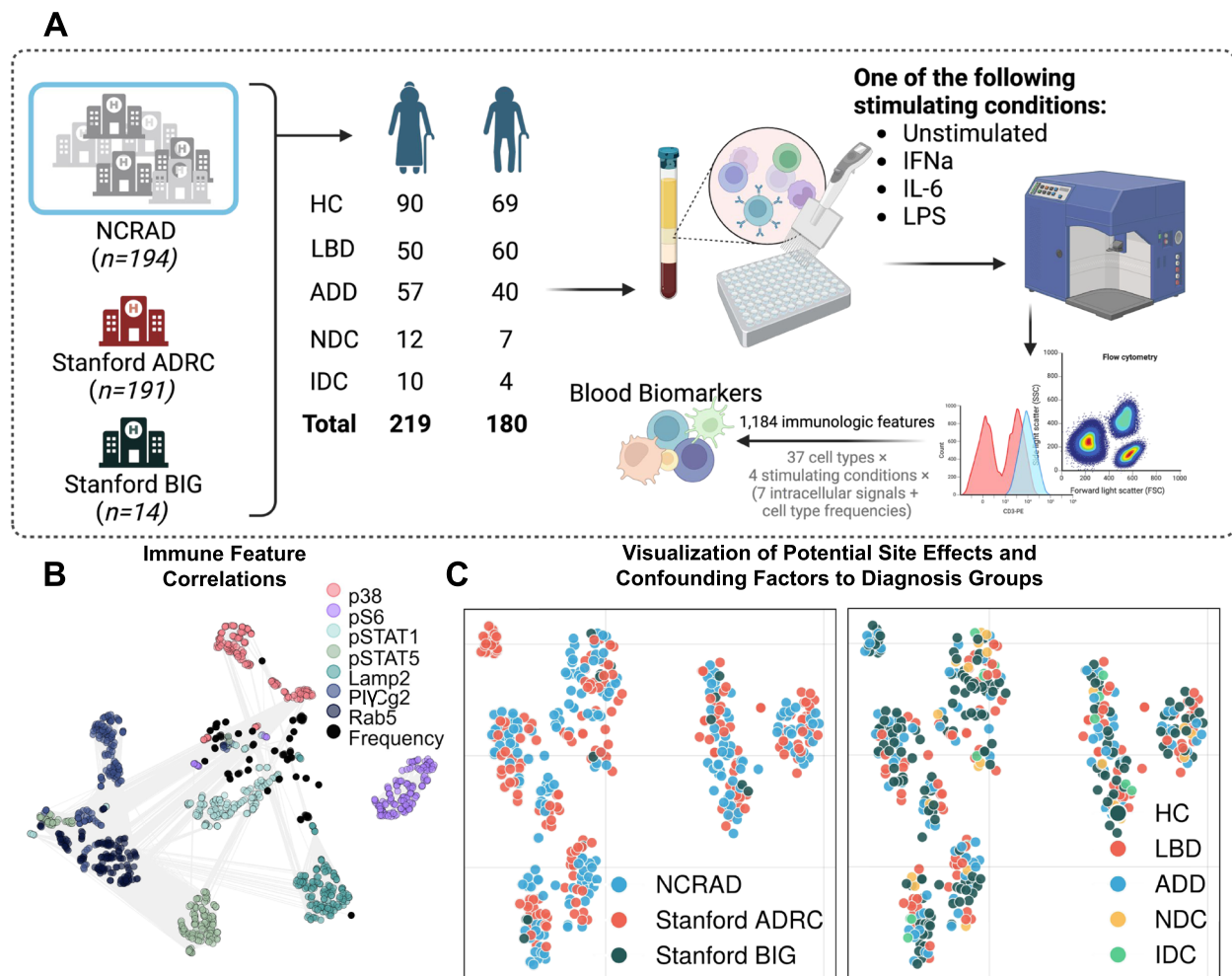


**Fig. 1** Overall Experiment and Resulting Immune Landscape. **A** Diagram of the experiment. PBMCs were collected from diagnosis groups at Stanford ADRC, Stanford BIG, and NCRAD, which in itself aggregated samples from multiple sites. This was followed by stimulating the PBMCs with one of three different canonical immune activators or vehicle control, immunolabelling for surface and intracellular markers, and measuring the cell-specific signals using flow cytometry. Single-cell signals were manually gated to different cell types, resulting in 1,184 immune features for each PBMC sample that were then used by machine learning for the identification of biomarkers. **B** A correlation network (edges represent Pearson's  $R > 0.7$ ) indicates that the immune landscape was mostly determined by the intracellular signals, i.e. the same intracellular signals tend to be correlated to each other despite different cell types and stimulating conditions. **C** The t-SNE plots suggest that there was not a strong effect by the site of sample collection (left), and that samples from different diagnosis groups were well distributed overall (right)

to power=1 at  $\alpha=0.05$  after Bonferroni adjustment; Fig. 2A), while predictions were essentially random for HC vs. ADD (AUROC=0.50 $\pm$ 0.05, AUPRC=0.39 $\pm$ 0.04, power<0.80 at adjusted- $\alpha=0.05$ ). It should be noted that random guess would yield an AUROC of 0.50, and an AUPRC equivalent to the prevalence of the positive class, which is displayed as patterned gray bars in all figures. The uneven distribution of LBD among sites could be concerning; however, even if the training and test set were split by site, instead of random cross-validation, or if only the Stanford cohort was included, the model still achieved high performance for HC vs. LBD

(AUROC=0.76 in Fig. 2B; AUROC=0.81 $\pm$ 0.08 in Fig. S3). Additionally, the model trained to predict HC-LBD yielded an AUROC of 0.55 $\pm$ 0.18 when transferred without retraining to predict batches. This indicates that the batch effect, if any, did not intervene with the diagnosis signals picked up by the model. This indicates that there was a generalizable pattern of PBMC response for participants with LBD regardless of clinical subgrouping. To ensure that these immune features were unique to LBD, the same HC vs. LBD model was used to predict ADD vs. LBD, NDC vs. LBD, and IDC vs. LBD without retraining. All of these comparisons resulted in high performance

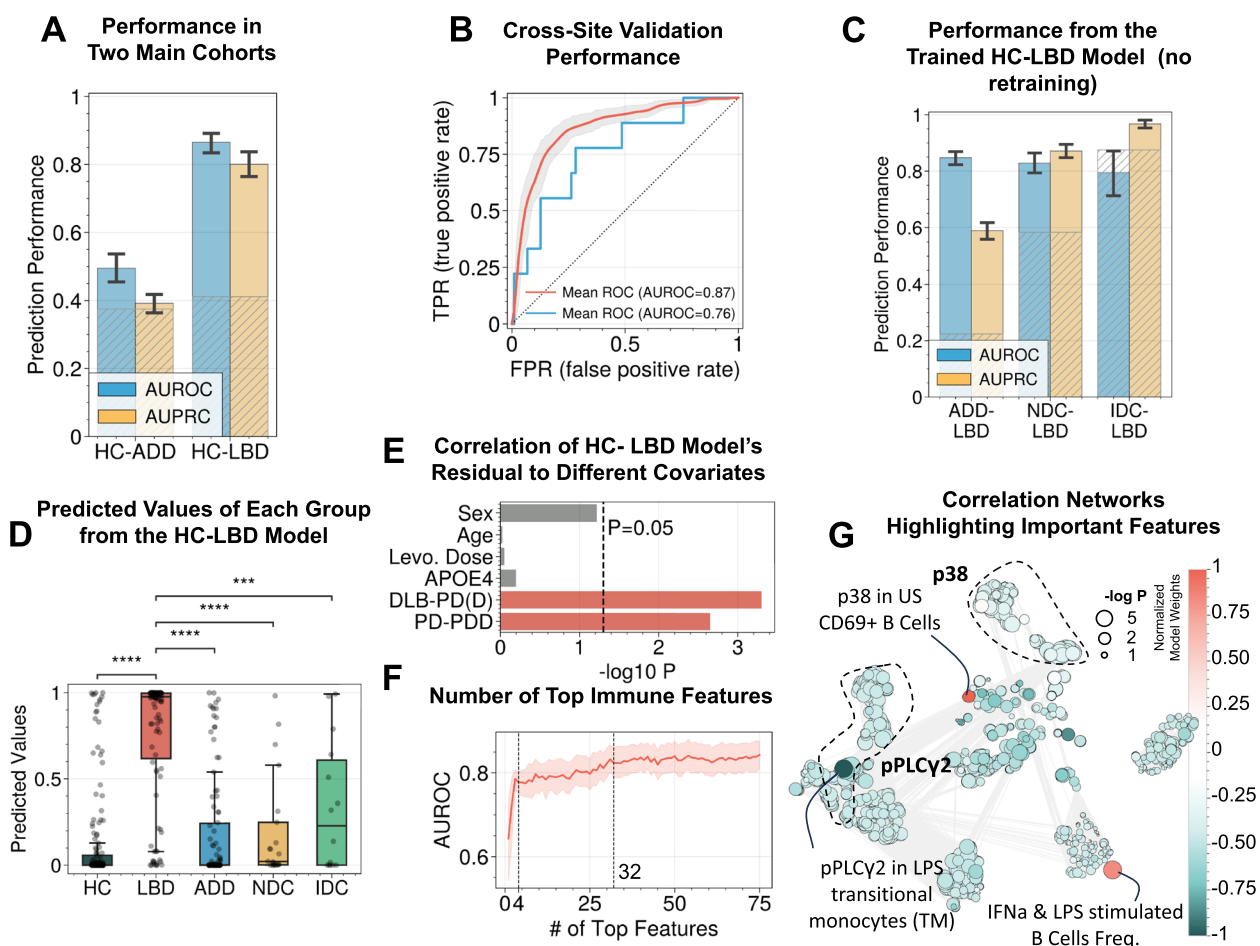


**Fig. 2** Models developed from multi-site data suggest peripheral biomarkers for LBD. **A** The model performance suggested good separation for HC vs. LBD, but not for HC vs. ADD. Note that a random guess baseline would yield an AUROC of 0.50 and an AUPRC equivalent to the prevalence of the positive class in the sample group, which are shown as patterned gray bars. **B** Performance using cross-site validation suggests the generalizability of the biomarkers. **C** Transferring the HC vs. LBD model (without retraining) to classify LBD from disease controls, including ADD, NDC, and IDC, yielded similarly high performance. **D** The predicted values from the HC vs. LBD model for all diagnosis groups show that the model is LBD-specific. **E** Model residual (errors from each prediction) did not significantly (M.W.U.  $P < 0.05$ ) vary with sex, age, Levodopa dosage, APOE  $\epsilon 4$  status, or PD vs. PDD. This indicates that the model performed equally well across these variables. In contrast, the model's residual varied for the DLB vs. PD/PDD group, suggesting that the performance of the DLB group differed from the PD/PDD group. **F** The required number of top immune features needed to achieve similar performance as all 1,184 features. **G** Correlation network highlighting the top features and the immune features with which they are correlated

with all AUROC above 0.79 (Fig. 2C). Neurodegenerative diseases commonly co-occur in older individuals [58]. While the NDC is an appropriate cohort to represent a group of these diseases for real-world implications, it should be noted that the group does not have sufficient granularity to compare with a specific disease subgroup. However, the achieved AUC of 0.83 (Fig. 2C) was strong and yielded a power of 1 and was still at a power of 0.97 (adjusted- $\alpha = 0.05$ ) even if we limit the control number to the same as the case number. Corresponding to these AUROC performances, Fig. 2D shows that the predicted values for LBD in the test set were significantly different

from all other diagnoses. Moreover, the residual of the model predictions (Fig. 2E) was not significantly correlated with sex, age, APOE  $\epsilon 4$  allele status, or Levodopa dosage; however, the model's residuals were significantly correlated with PD vs. PDD or DLB vs. PD/PDD, indicating that the model performed equally well across these major variables except within the LBD diagnosis group.

Model reduction indicated that only the top 4 immune features were necessary to achieve a satisfactory prediction performance, and 32 features would yield similar performance as using all 1,184 immune features (Fig. 2F).

The top 4 immune features for LBD were highlighted in the immune feature correlation network (Fig. 2G). They include reduced pPLC $\gamma$ 2 response from LPS-stimulated CD14+CD16+ monocytes, elevated p38 response from unstimulated CD69+B cells, and frequency of IFN $\alpha$  and LPS-stimulated B cells.

Due to the high correlations among immune features, the model may only select a few representative ones, and interpretation from the model alone may leave out other important biological features. For this reason, other immune features were investigated from a univariate perspective. Heatmaps of the correlations between the top intracellular signals and LBD diagnosis show

cell type-specific signals, including: reduced expression of pPLC $\gamma$ 2 in CD69+ NK cells, transitional monocytes (TM), and CD11b+HLA-DR+ TM; reduced expression of pSTAT5 in multiple CD4+ cells; and elevated expression of p38 in multiple CD4+ and CD8+ cells in participants with LBD compared to HC (Fig. 3A). Note that because neurodegenerative disease groups and HC are sex- and age-matched, adjusting these correlations by sex and age did not change any signals for the diagnoses (Fig. S4). Notably, these signals were significantly different between LBD vs. HC and LBD vs. ADD but not between LBD vs. NDC or LBD vs. IDC (Fig. 3B),

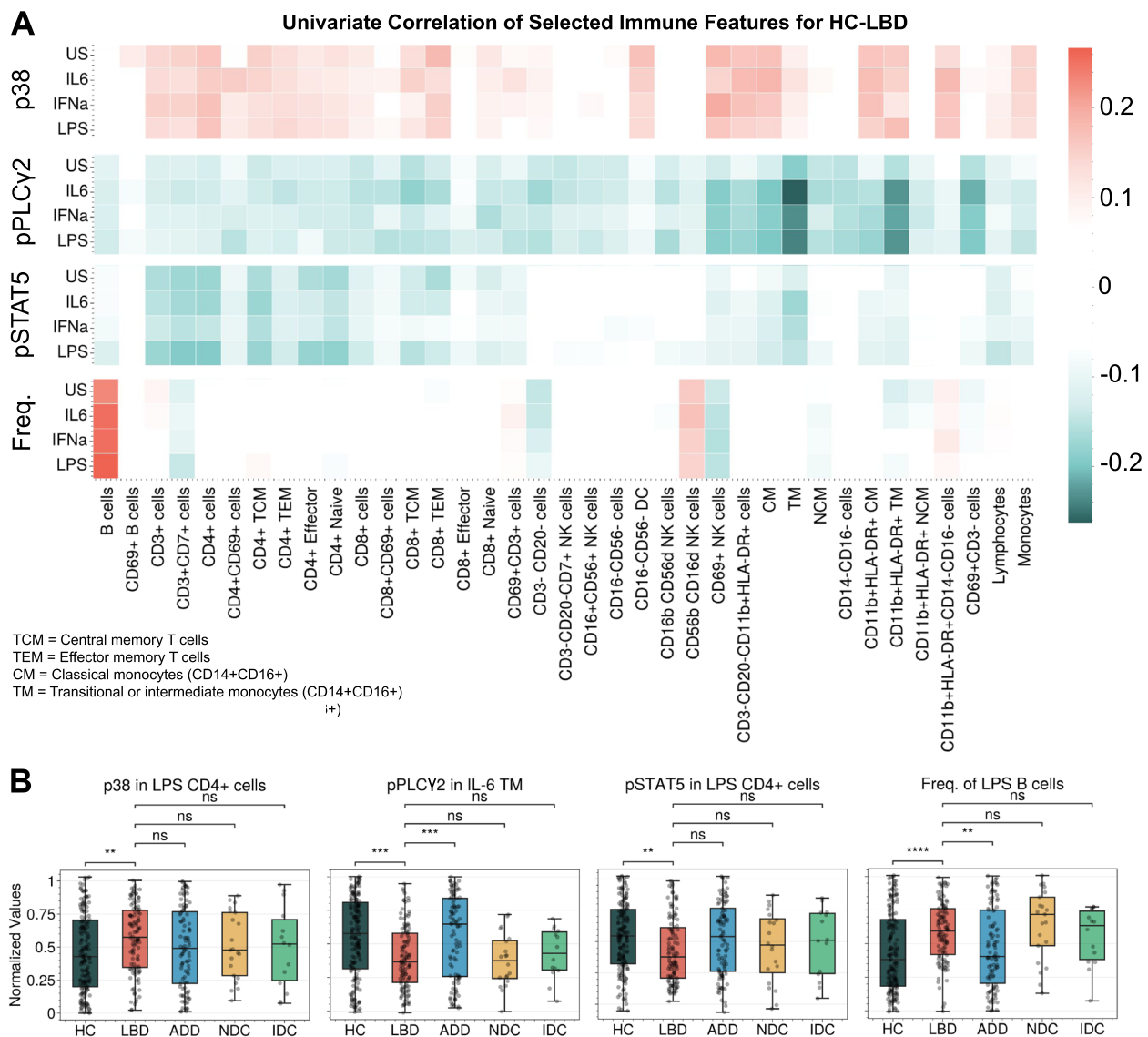


**Fig. 3** Strong signals for HC vs. LBD were cell-type specific. **A** The heatmap of selected intracellular signals (or frequency) from all cell types shows the cell types with the strongest correlations to LBD. **B** Examples of the top univariate immune features

highlighting the need to integrate multiple immune features and non-linear models.

**Differential signals separating DLB, PD, and PDD with cognitive impairment**

So far, we have determined a unique peripheral immune pattern for participants with LBD compared to HC, ADD, and other neurodegenerative or autoimmune disease controls. However, as noted above, participants with LBD are a mix of individuals with three different clinical diagnoses (PD, PDD, and DLB) that can be difficult to distinguish clinically with precision and that can merge over time. Our results show that each of these diagnostic subgroups of LBD can mostly be separated from HC moderately well with the exception of HC vs. DLB which exhibited the lowest performance (AUROC=0.62–0.89, AUPRC=0.29–0.71, power=0.40–1 at adjusted- $\alpha$ =0.05;

Fig. 4A). Transferring these models without retraining to cross-predict among themselves, e.g. PD vs. PDD or PDD vs. DLB, exhibited moderately low performance (AUROC=0.54–0.65, power<0.80 at adjusted- $\alpha$ =0.05; Fig. 4B). The moderate classification performance indicates that PD, PDD, and DLB share some critical PBMC immune responses in addition to the known shared neuropathological features. Interestingly, the model transfer to classify each LBD subgroup vs. ADD resulted in high AUROC (>0.84) for both PD and PDD (Fig. 4B) but not as high for ADD vs. DLB (AUROC=0.62), perhaps because of the well-described comorbidity between DLB and AD neurodegenerative change in the majority of people diagnosed clinically with DLB [45].

From a univariate perspective when compared with HC, PDD exhibited the highest number of statistically significant immune features (M.W.U.  $P < 0.01$ ), and only

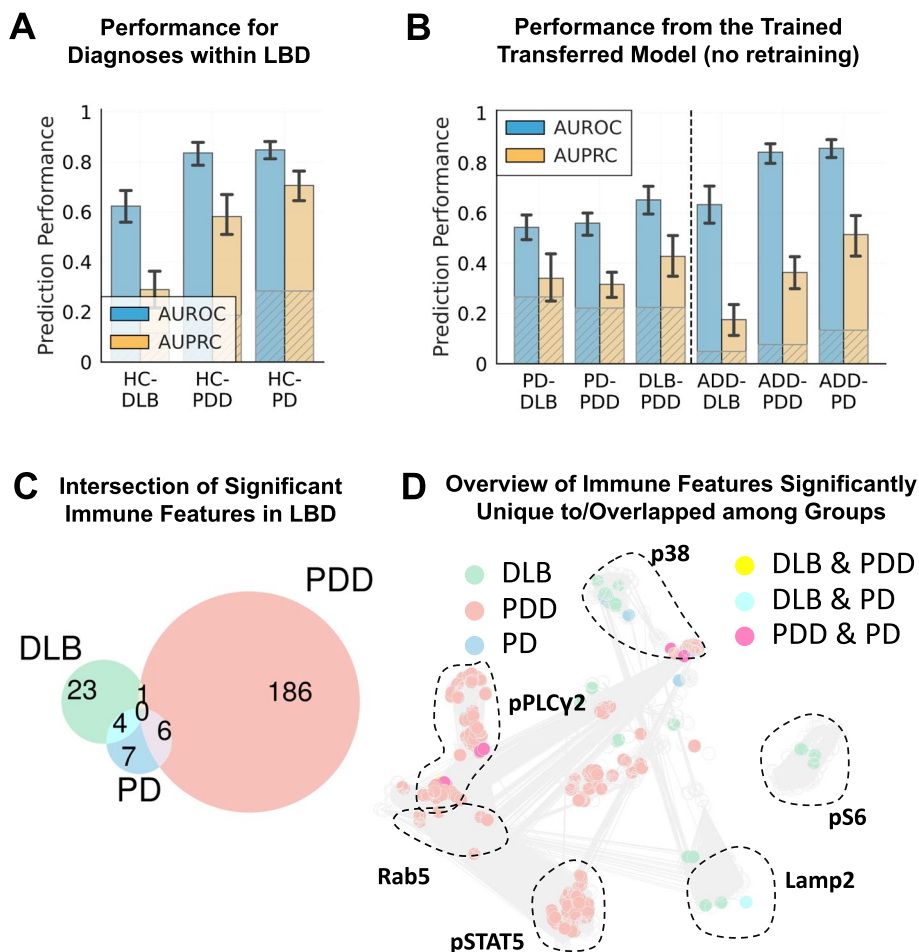


**Fig. 4** All subgroups within LBD can be separated from HC, but not among themselves. **A** Model performance of three separate models each developed for classifying HC from each of the subgroups within LBD, including DLB, PDD, and PD. **B** The performance of the same models (without retraining) classifying among each of the subgroups and all of them vs. AD. **C** The Venn diagrams of significant immune features for each group (M.W.U.  $P < 0.01$ ) indicated small overlapping features among them. **D** The correlation network shows which immune features were unique to or overlapping between DLB, PDD, and PD



a handful of these was shared by PD and DLB (Fig. 4C). From the univariate intracellular signals for LBD in the previous section, elevated p38 responses were uniquely associated with a diagnosis of PD with or without dementia (Fig. 4D), while most of the reduced pPLC $\gamma$ 2 response and reduced expression of pSTAT5 were uniquely associated with PDD only.

Cognitive exams in multiple domains are predictive of cognitive status in LBD [59], and together with motor exams and clinicians' judgment, were the source for deriving a clinical diagnosis. We also tested if the immune features can predict any of the 18 neuropsychological battery test scores in the cases where the data were available, such as trail making or MMSE, or any of the 23 motor examinations from the UPDRS among participants with LBD. Our results show moderately low performance, indicating that the selected immune features were not specific to these measurements in LBD participants (Fig. S5 & S6).

#### Overlap between LBD and other common comorbidities

Several diseases and conditions that are not primarily associated with neurodegeneration tend to increase or lower the risk of dementia and PD. Examples of these include arthritis [60], diabetes [61], hypercholesterolemia [62], hypertension [63], REM sleep disorder [64], sleep apnea [65], traumatic brain injury (TBI) [66], and vitamin B12 deficiency (VB12DEF) [67]. This section aims to investigate whether the peripheral immune biomarkers discovered above had links with these common comorbidities. In the cases where comorbidities data were available in our sample set, individuals with these comorbidities were almost equally split among HC, ADD, or

LBD (Fig. 5A) except for diabetes, which only occurred in HC and AD, and REM sleep disorders, which only occurred in LBD.

Model transfers were conducted where the model trained to separate HC vs. LBD was used, without retraining, to classify each of the comorbidities. We found that only REM sleep disorder (REMDIS) yielded moderately good performance (AUROC=0.73, power=0.98 at adjusted- $\alpha$ =0.05; Fig. 5B). We also investigated if we could identify signatures in each comorbidity individually. TBI and VB12DEF achieved the highest AUROC (AUROC=0.62 and 0.61, respectively) but both at power < 0.8 at  $\alpha$ =0.05. This low performance could be attributed to insufficient case numbers to individually develop an effective machine learning model (Fig. S7). Even though all known comorbidity data were included (no exclusion), their numbers were still limited due to their availability only in newer NACC data versions and above [68] (Table S2). Figure 5C shows the feature overlaps between REMDIS and LBD from a univariate test (features with AUROC>0.6). This could stem from the fact that all participants with REMDIS in our cohort had LBD, while only about 30% of participants without REMDIS had LBD; a future dedicated REMDIS cohort would be needed to decouple their confounding effects. In conclusion, our results suggest that the identified LBD signals were likely only weakly influenced by these comorbidities, except for the confounding REMDIS.

#### Discussion

Human genetic, pathologic, imaging, and biochemical data as well as results from experimental models have linked neuroinflammation with the initiation or

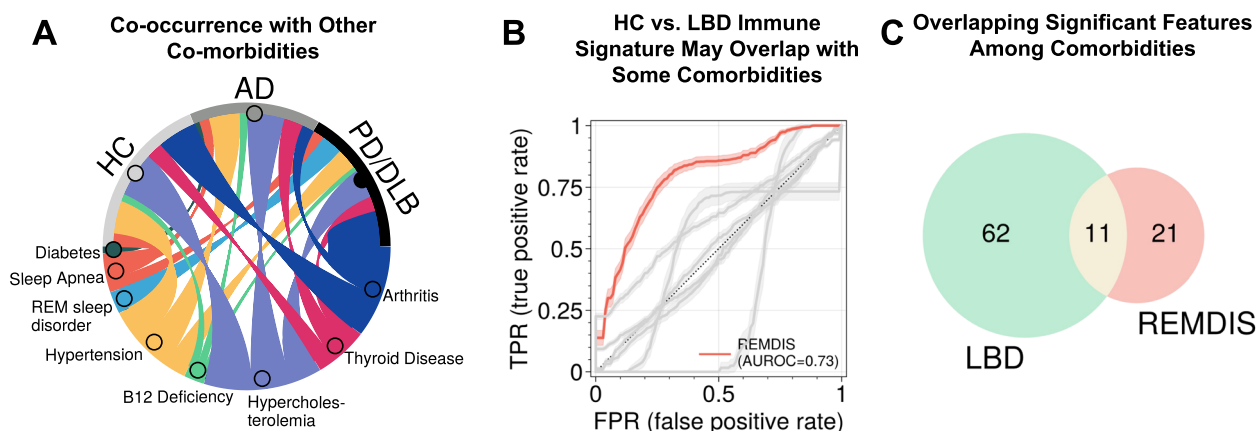


**Fig. 5** The identified LBD biomarkers did not have overlapping biological pathways with common non-neurodegenerative comorbidities. **A** A chord diagram displaying LBD, ADD, or HC co-occurrence with other comorbidities. Note that TBI was also included but due to a low number of cases ( $n=6$ ), it is now shown in the plot. **B** Model performances (AUROC) for all comorbidities using model transfer from HC vs. LBD showing that it can also classify REMDIS. **C** The Venn diagrams of significantly overlapped immune features among groups (M.W.U.  $P < 0.01$ )

progression of prevalent age-related neurodegenerative diseases. Among these, the LBD spectrum, PD, PDD, and DLB, have been most strongly linked to events in the periphery as potential contributing mechanisms that impact the brain [69]. Here we tested the hypothesis that cell-specific immune responses by PBMCs might be associated with LBD diagnosis, highlighting potential peripheral biomarkers and possibly illuminating mechanisms of disease. Our multisite study design included PBMCs from 399 participants from five diagnostic groups (HC, LBD, ADD, and NDC as controls for non-specific changes occurring with debilitation from neurodegenerative diseases, and IDC to control for non-specific changes occurring with immune-mediated diseases) that were investigated in basal state or following stimulation by canonical immune activators to generate 1,184 molecular features per individual. These rich immune response data were coupled with extensive clinical annotation and analyzed by machine learning techniques.

Our major finding was that, within the context of our stimulants and multiplex panel, only 4 immune features were necessary to achieve similar prediction performance for LBD as all immune features; these were: reduced pPLC $\gamma$ 2 response from LPS-stimulated transitional monocytes, elevated p38 response from unstimulated CD69+B cells, and increased frequency of IFN $\alpha$  and LPS stimulated B cells. Together these data suggest a broad alteration in peripheral immune response in participants with LBD that is distinct from other neurodegenerative and autoimmune diseases, and that involves monocytes and lymphocytes, establishing pathologic relevance for these immune response changes in people with LBD. Determining the pathogenic mechanisms by which these stimulant- and cell-specific immune responses may or may not directly contribute to LBD-type neurodegeneration will require means of selectively manipulating each in isolation or combinations in model systems that faithfully reflect the human immune system and mechanisms of neurodegeneration in LBD. Future work may combine validated markers of immune response with markers of other pathological processes central to LBD pathogenesis, like seed propagation assays for alpha-synuclein, to gain a more comprehensive view of disease initiation and progression.

On top of identified features from the model, univariate statistical analysis results highlight three immune response features that are strongly characteristic of PBMCs from people diagnosed with LBD: reduced pSTAT5 in CD4+ subset and reduced pPLC $\gamma$ 2 response and elevated p38 response in subsets of NK cells and TM cells. Our localization of elevated p38 response to lymphocytes in people with LBD suggests that this may be a feature of a subset of lymphocytes that traffic into the

brain as immune master regulators [69]. Additionally, p38 is extensively related to gut immunity, inflammation, and aging [70–72]; gut physiology has been implicated by many studies as a potential contributor to LBD [73]. PLC $\gamma$ 2 is highly expressed in immune cells including microglia, and gain-of-function mutations in *PLCG2* cause autoimmune diseases [37–40]. A nonsynonymous variant in *PLCG2* is associated with reduced risk of ADD, DLB, and frontotemporal dementia, suggesting a broad influence on the mechanisms of neurodegeneration, most likely neuroinflammation [33, 74]. Our results showed reduced phosphorylation of PLC $\gamma$ 2, the molecular mechanism of its activation, in peripheral monocytes and other PBMCs of participants with LBD, thereby aligning with genetic data associating less active PLC $\gamma$ 2 with increased risk of LBD. In a previous single-site study we identified reduced pPLC $\gamma$ 2 in a small group of ADD participants [25]; however this result did not generalize to the current multisite study with 4 times more ADD samples. Together, these findings suggest a broad influence of PLC $\gamma$ 2 activation in peripheral immunocompetent cells in multiple forms of neurodegenerative disease but most robustly in LBD.

The medical and pathological distinctiveness of the LBD subgroups, PD, PDD, and LBD, is a decades-long debate [5]. We sought to determine the extent to which peripheral immune responses as measured here may potentially point to LBD subgroup-specific features. We observed low model prediction performance among PD, PDD, and DLB suggesting that at least as determined by our multiplex panel, PBMC immune responses are similar among the three subgroups. Further univariate analysis suggested that increased signaling through pPLC $\gamma$ 2 and pSTAT might be a peripheral immune feature specific to PDD and not PD or DLB. Interestingly, despite being predictive of LBD and its subgroups, peripheral immune responses were not strongly predictive of performance on neuropsychological tests or consensus motor evaluation, nor were they associated with other medical conditions shown to modulate the risk of LBD. We speculate that the detected peripheral immune response in LBD subgroups may be a consequence of LBD-type neurodegeneration or may reveal an underlying inherited or acquired trait that renders a person more vulnerable to developing LBD without being directly involved in the extent of neurodegeneration.

Our study has limitations. While the overall sample size is adequate, some of the LBD subgroup sizes were small and lacked neuroimaging, biomarkers, or pathologic validation of clinical diagnosis. For these reasons, LBD subgroup comparisons should be considered preliminary. Similarly, our analyses of common comorbidities remain preliminary due to the limited availability of data

(Table S2). Additionally, data on recent infectious status/febrile processes in our participants were unavailable. Also, the multisite samples were majority Caucasian or Asian representing a national deficit in sample diversity among these diseases that is currently being addressed. With these limitations in mind, our quantification of PBMC immune response from multisite research participants yielded a unique pattern for LBD compared to HC, multiple related neurodegenerative diseases, and autoimmune diseases thereby highlighting potential biomarkers and insights into mechanisms of LBD.

## Conclusion

This study demonstrates that peripheral immune responses, particularly those detected in PBMCs, exhibit distinct patterns in participants with Lewy body disease (LBD) compared to healthy controls and other neurodegenerative or autoimmune conditions. The identified immune features, including pPLC $\gamma$ 2, p38, and pSTAT5 signals from specific cell subsets and activations, offer potential biomarkers and insights into the mechanistic underpinnings of LBD pathogenesis. These findings contribute to a deeper understanding of LBD and may pave the way for the development of novel diagnostic tools to guide the stratification of individuals with LBD enrolled in trials or to target immunomodulatory interventions in people with LBD.

## Abbreviations

PBMC	Peripheral mononuclear cell
LBD	Lewy body disease
PD	Parkinson's Disease without dementia
PDD	Parkinson's Disease with dementia
DLB	Dementia with Lewy bodies
ADD	Alzheimer's disease dementia
HC	Healthy controls
NDC	Neurodegenerative disease controls
IDC	Immune disease controls
LPS	Lipopolysaccharide
IL-6	Interleukin-6
IFN $\alpha$	Interferon-alpha
AUROC	Area under the receiving operating characteristic
AUPRC	Area under precision-recall curve
LGBM	Light gradient-boosting machine
ADRC	Alzheimer's Disease Research Center
NCRAD	National Centralized Repository for Alzheimer's Disease and Related Dementias
BIG	Stanford BIG Project
HTS	High throughput sampler
HIMC	Human Immune Monitoring Center

## Supplementary Information

The online version contains supplementary material available at <https://doi.org/10.1186/s13024-024-00748-2>.

Supplementary Material 1.

## Acknowledgements

Annotated IDC samples are made available from the Project BIG biorepository.

## Authors' contributions

Conceptualization, T.P. and T.J.M.; Methodology, T.P., C.R.G., K.M., H.T.M., F.X., C-H.S., N.A., and T.M.; Investigation, T.P., N.S., K.M., E.J.F., S.C.P., and S.Y.W.; Visualization, T.P., C.E., A.P.; Writing – Original Draft, T.P. and T.J.M.; Writing – Review & Editing, E.B., D.H., B.C., M.R., P.C., N.A., and K.S.M.; Data Curation, D.C., L-J.H., T.P., K.M.; Funding Acquisition, T.P., E.J.F., T.J.M., N.A., K.L.M., K.S.M.; Resources, D.C., L-J.H., J.E.D., and L.B.K.; Supervision, T.P., N.A., and T.J.M.

## Funding

Samples from the National Centralized Repository for Alzheimer's Disease and Related Dementias (NCRAD), which receives government support under a cooperative agreement grant (U24 AG21886) awarded by the National Institute on Aging (NIA), were used in this study. We thank contributors who collected samples used in this study, as well as participants and their families, whose help and participation made this work possible. Support for this research related to healthy controls, ADD, and LBD samples has also been kindly provided by the Stanford ADRC (P30 AG066515) and the Pacific UDALL Center. Support for this research related to autoimmune disease controls has been kindly provided by the Project BIG Fund and the Garrett Immunology Research Fund. Flow cytometry and initial analysis thereof were performed in the Stanford Human Immune Monitoring Center (HIMC).

This work was supported by NIA RF1AG077443 (T.J.M., N.A.), NIGMS 5T32GM089626 (P.C.). Funding also provided for by the Alzheimer's Drug Discovery Foundation (ADDF) Diagnostics Accelerator, a fund set up in collaboration with Bill Gates and other philanthropic partners. The initiative seeks to accelerate the development of affordable and accessible biomarkers to diagnose Alzheimer's disease and related dementias, and to advance the development of more targeted treatments. To learn more about the initiative visit the website at: (AlzDiscovery.org).

## Availability of data and materials

Anonymized data, including singlet live cell data (fcs format), gated median value data (csv format), and the associated metadata (csv format) will be made available on request to qualified researchers who have institutional review board approval and a Data Use Agreement at relevant sites.

## Declarations

### Ethics approval and consent to participate

All participants provided written informed consent to participate in the study, which followed protocols approved by the Stanford Institutional Review Board.

### Consent for publication

N/A.

### Competing interests

The authors declare no competing interests.

### Author details

<sup>1</sup>Department of Pathology, Stanford University, Stanford, CA, USA. <sup>2</sup>Department of Anesthesiology, Perioperative and Pain Medicine, Stanford University, Stanford, CA, USA. <sup>3</sup>Department of Biomedical Data Science, Stanford University, Stanford, CA, USA. <sup>4</sup>Institute for Immunity, Transplantation and Infection, Stanford University, Stanford, CA, USA. <sup>5</sup>Department of Pediatrics, Stanford University, Stanford, CA, USA. <sup>6</sup>Department of Neurology and Neurological Sciences, Stanford University, Stanford, CA, USA.

Received: 6 February 2024 Accepted: 22 July 2024

Published online: 01 August 2024

## References

1. Yi S, Wang L, Wang H, Ho MS, Zhang S. Pathogenesis of  $\alpha$ -synuclein in Parkinson's Disease: from a neuron-glia crosstalk perspective. *Int J Mol Sci*. 2022;23:14753.
2. Stefanis L.  $\alpha$ -Synuclein in Parkinson's disease. *Cold Spring Harb Perspect Med*. 2012;2:a009399.

3. Meade RM, Fairlie DP, Mason JM. Alpha-synuclein structure and Parkinson's disease – lessons and emerging principles. *Mol Neurodegener.* 2019;14:29.
4. Kim WS, Kågedal K, Halliday GM. Alpha-synuclein biology in Lewy body diseases. *Alzheimers Res Ther.* 2014;6:73.
5. Weintraub D. What's in a name? The time has come to unify Parkinson's disease and dementia with Lewy bodies. *Mov Disord.* 2023;38:1977–81.
6. Phongpreecha T, Gajera CR, Liu CC, Vijayaragavan K, Chang AL, Becker M, et al. Single-synapse analyses of Alzheimer's disease implicate pathologic tau, DJ1, CD47, and ApoE. *Sci Adv.* 2021;7:eabk0473.
7. Tansey MG, Romero-Ramos M. Immune system responses in Parkinson's disease: Early and dynamic. *Eur J Neurosci.* 2019;49:364–83.
8. Hirsch EC, Standaert DG. Ten unsolved questions about neuroinflammation in Parkinson's disease. *Mov Disord.* 2021;36:16–24.
9. Pajares M, I. Rojo A, Manda G, Boscá L, Cuadrado A. Inflammation in Parkinson's disease: mechanisms and therapeutic implications. *Cells.* 2020;9:1687.
10. Tansey MG, Wallings RL, Houser MC, Herrick MK, Keating CE, Joers V. Inflammation and immune dysfunction in Parkinson disease. *Nat Rev Immunol.* 2022;22:657–73.
11. Tan E-K, Chao Y-X, West A, Chan L-L, Poewe W, Jankovic J. Parkinson disease and the immune system — associations, mechanisms and therapeutics. *Nat Rev Neurol.* 2020;16:303–18.
12. Harms AS, Ferreira SA, Romero-Ramos M. Periphery and brain, innate and adaptive immunity in Parkinson's disease. *Acta Neuropathol (Berl).* 2021;141:527–45.
13. Harms AS, Yang Y-T, Tansey MG. Central and peripheral innate and adaptive immunity in Parkinson's disease. *Sci Transl Med.* 2023;15:eak3225.
14. Gate D, Saligrama N, Leventhal O, Yang AC, Unger MS, Middeldorp J, et al. Clonally expanded CD8 T cells patrol the cerebrospinal fluid in Alzheimer's disease. *Nature.* 2020;577:399–404.
15. Rocha NP, Assis F, Scalzo PL, Vieira ÉLM, Barbosa IG, de Souza MS, et al. Reduced Activated T Lymphocytes (CD4+CD25+) and Plasma Levels of Cytokines in Parkinson's Disease. *Mol Neurobiol.* 2018;55:1488–97.
16. Cen L, Yang C, Huang S, Zhou M, Tang X, Li K, et al. Peripheral lymphocyte subsets as a marker of Parkinson's disease in a Chinese population. *Neurosci Bull.* 2017;33:493–500.
17. Niwa F, Kuriyama N, Nakagawa M, Imanishi J. Effects of peripheral lymphocyte subpopulations and the clinical correlation with Parkinson's disease. *Geriatr Gerontol Int.* 2012;12:102–7.
18. Chen Y, Qi B, Xu W, Ma B, Li L, Chen Q, et al. Clinical correlation of peripheral CD4+ cell sub-sets, their imbalance and Parkinson's disease. *Mol Med Rep.* 2015;12:6105–11.
19. Kustrimovic N, Rasini E, Legnaro M, Marino F, Cosentino M. Expression of dopaminergic receptors on human CD4+ T lymphocytes: flow cytometric analysis of naive and memory subsets and relevance for the neuroimmunology of neurodegenerative disease. *J Neuroimmune Pharmacol.* 2014;9:302–12.
20. Su Y, Shi C, Wang T, Liu C, Yang J, Zhang S, et al. Dysregulation of peripheral monocytes and pro-inflammation of alpha-synuclein in Parkinson's disease. *J Neurol.* 2022;269:6386–94.
21. Hasegawa Y, Inagaki T, Sawada M, Suzumura A. Impaired cytokine production by peripheral blood mononuclear cells and monocytes/macrophages in Parkinson's disease. *Acta Neurol Scand.* 2000;101:159–64.
22. Bessler H, Djaldetti R, Salman H, Bergman M, Djaldetti M. IL-1 $\beta$ , IL-2, IL-6 and TNF- $\alpha$  production by peripheral blood mononuclear cells from patients with Parkinson's disease. *Biomed Pharmacother.* 1999;53:141–5.
23. Reale M, Iarlori C, Thomas A, Gambi D, Perfetti B, Di Nicola M, et al. Peripheral cytokines profile in Parkinson's disease. *Brain Behav Immun.* 2009;23:55–63.
24. Li Y, Yang Y, Zhao A, Luo N, Niu M, Kang W, et al. Parkinson's disease peripheral immune biomarker profile: a multicentre, cross-sectional and longitudinal study. *J Neuroinflammation.* 2022;19:116.
25. Phongpreecha T, Fernandez R, Mrdjen D, Culos A, Gajera CR, Wawro AM, et al. Single-cell peripheral immunoprofiling of Alzheimer's and Parkinson's diseases. *Sci Adv.* 2020;6:eabd5575.
26. Grayson JM, Short SM, Lee CJ, Park N, Marsac C, Sette A, et al. T cell exhaustion is associated with cognitive status and amyloid accumulation in Alzheimer's disease. *Sci Rep.* 2023;13:15779.
27. Fernández Zapata C, Giacomello G, Spruth EJ, Middeldorp J, Gallaccio G, Dehlinger A, et al. Differential compartmentalization of myeloid cell phenotypes and responses towards the CNS in Alzheimer's disease. *Nat Commun.* 2022;13:7210.
28. Fiala M, Lin J, Ringman J, Kermani-Arab V, Tsao G, Patel A, et al. Ineffective phagocytosis of amyloid- $\beta$  by macrophages of Alzheimer's disease patients. *J Alzheimers Dis.* 2005;7:221–32.
29. Vasanthekha R, Priyanka HP, Nair RS, Hima L, Pratap UP, Srinivasan AV, et al. Alterations in immune responses are associated with dysfunctional intracellular signaling in peripheral blood mononuclear cells of men and women with mild cognitive impairment and Alzheimer's disease. *Mol Neurobiol.* 2023 [cited 2023 Dec 20]. <https://doi.org/10.1007/s12035-023-03764-3>
30. Cook DA, Kannarkat GT, Cintron AF, Butkovich LM, Fraser KB, Chang J, et al. LRRK2 levels in immune cells are increased in Parkinson's disease. *Npj Park Dis.* 2017;3:1–12.
31. Gopinath A, Mackie P, Hashimi B, Buchanan AM, Smith AR, Bouchard R, et al. DAT and TH expression marks human Parkinson's disease in peripheral immune cells. *Npj Park Dis.* 2022;8:1–14.
32. Jiang S-S, Wang Y-L, Xu Q-H, Gu L-Y, Kang R-Q, Yang W-Y, et al. Cytokine and chemokine map of peripheral specific immune cell subsets in Parkinson's disease. *Npj Park Dis.* 2023;9:1–9.
33. van der Lee SJ, Conway OJ, Jansen I, Carrasquillo MM, Kleineidam L, van den Akker E, et al. A nonsynonymous mutation in PLCG2 reduces the risk of Alzheimer's disease, dementia with Lewy bodies and frontotemporal dementia, and increases the likelihood of longevity. *Acta Neuropathol (Berl).* 2019;138:237–50.
34. Obergasteiger J, Frapporti G, Pramstaller PP, Hicks AA, Volta M. A new hypothesis for Parkinson's disease pathogenesis: GTPase-p38 MAPK signaling and autophagy as convergence points of etiology and genomics. *Mol Neurodegener.* 2018;13:40.
35. Klaver AC, Coffey MP, Aasly JO, Loeffler DA. CSF lamp2 concentrations are decreased in female Parkinson's disease patients with LRRK2 mutations. *Brain Res.* 2018;1683:12–6.
36. Marx FP, Soehn AS, Berg D, Melle C, Schiesling C, Lang M, et al. The proteasomal subunit S6 ATPase is a novel synphilin-1 interacting protein—implications for Parkinson's disease. *FASEB J.* 2007;21:1759–67.
37. Ombrello MJ, Remmers EF, Sun G, Freeman AF, Datta S, Torabi-Parizi P, et al. Cold Urticaria, Immunodeficiency, and Autoimmunity Related to PLCG2 Deletions. *N Engl J Med.* 2012;366:330–8.
38. Schade A, Walliser C, Wist M, Haas J, Vatter P, Kraus JM, et al. Cool-temperature-mediated activation of phospholipase C- $\gamma$ 2 in the human hereditary disease PLAID. *Cell Signal.* 2016;28:1237–51.
39. Yu P, Constien R, Dear N, Katan M, Hanke P, Bunney TD, et al. Autoimmunity and Inflammation due to a gain-of-function mutation in phospholipase C $\gamma$ 2 that specifically increases external Ca $^{2+}$  entry. *Immunity.* 2005;22:451–65.
40. Zhou Q, Lee G-S, Brady J, Datta S, Katan M, Sheikh A, et al. A hypermorphic missense mutation in PLCG2, encoding phospholipase C $\gamma$ 2, causes a dominantly inherited autoinflammatory disease with immunodeficiency. *Am J Hum Genet.* 2012;91:713–20.
41. Xie Z, Smith CJ, Van Eldik LJ. Activated glia induce neuron death via MAP kinase signaling pathways involving JNK and p38. *Glia.* 2004;45:170–9.
42. Jeohn G-H, Cooper CL, Wilson B, Chang RCC, Jang K-J, Kim H-C, et al. p38 MAP Kinase is involved in lipopolysaccharide-induced dopaminergic neuronal cell death in rat mesencephalic neuron-glia cultures. *Ann NY Acad Sci.* 2002;962:332–46.
43. Uniform Data Set version 3 | National Alzheimer's Coordinating Center [Internet]. [cited 2022 Jan 4]. Available from: <https://naccdata.org/data-collection/forms-documentation/uds-3>
44. Litvan I, Bhatia KP, Burn DJ, Goetz CG, Lang AE, McKeith I, et al. SIC Task Force appraisal of clinical diagnostic criteria for parkinsonian disorders. *Mov Disord.* 2003;18:467–86.
45. McKeith IG, Boeve BF, Dickson DW, Halliday G, Taylor J-P, Weintraub D, et al. Diagnosis and management of dementia with Lewy bodies: Fourth consensus report of the DLB Consortium. *Neurology.* 2017;89:88–100.
46. McKhann GM, Knopman DS, Chertkow H, Hyman BT, Jack CR Jr, Kawas CH, et al. The diagnosis of dementia due to Alzheimer's disease: Recommendations from the National Institute on Aging-Alzheimer's Association workgroups on diagnostic guidelines for Alzheimer's disease. *Alzheimers Dement.* 2011;7:263–9.
47. Mesulam MM. Primary progressive aphasia — a language-based dementia. *N Engl J Med.* 2003;349:1535–42.

48. Menon DK, Schwab K, Wright DW, Maas AI, Demographics and Clinical Assessment Working Group of the International and Interagency Initiative toward Common Data Elements for Research on Traumatic Brain Injury and Psychological. Health position statement: definition of traumatic brain injury. *Arch Phys Med Rehabil.* 2010;91:1637–40.
49. Thompson AJ, Banwell BL, Barkhof F, Carroll WM, Coetzee T, Comi G, et al. Diagnosis of multiple sclerosis: 2017 revisions of the McDonald criteria. *Lancet Neurol.* 2018;17:162–73.
50. Fernandez R, Maecker H. Cytokine-stimulated phosphoflow of whole blood using CyTOF mass cytometry. *Bio-Protoc.* 2015;5:e1495.
51. Krutzik PO, Irish JM, Nolan GP, Perez OD. Analysis of protein phosphorylation and cellular signaling events by flow cytometry: techniques and clinical applications. *Clin Immunol.* 2004;110:206–21.
52. Krutzik PO, Trejo A, Schulz KR, Nolan GP. Phospho Flow Cytometry Methods for the Analysis of Kinase Signaling in Cell Lines and Primary Human Blood Samples. In: Hawley TS, Hawley RG, editors. *Flow Cytom Protoc* [Internet]. Totowa: Humana Press; 2011 [cited 2024 Jun 22]. p. 179–202. Available from: [https://doi.org/10.1007/978-1-61737-950-5\\_9](https://doi.org/10.1007/978-1-61737-950-5_9)
53. Behdenna A, Colange M, Haziza J, Gema A, Appé G, Azencott C-A, et al. pyComBat, a Python tool for batch effects correction in high-throughput molecular data using empirical Bayes methods [Internet]. *bioRxiv*; 2023 [cited 2023 Nov 19]. p. 2020.03.17.995431. Available from: <https://www.biorxiv.org/content/10.1101/2020.03.17.995431v3>
54. Müller C, Schillert A, Röthemeier C, Trégouët D-A, Proust C, Binder H, et al. Removing batch effects from longitudinal gene expression - quantile normalization plus ComBat as best approach for microarray transcriptome data. *PLoS ONE.* 2016;11:e0156594.
55. Culos A, Tsai AS, Stanley N, Becker M, Ghaemi MS, McIlwain DR, et al. Integration of mechanistic immunological knowledge into a machine learning pipeline improves predictions. *Nat Mach Intell.* 2020;2:619–28.
56. Stanley N, Stelzer IA, Tsai AS, Fallahzadeh R, Ganio E, Becker M, et al. VoPo leverages cellular heterogeneity for predictive modeling of single-cell data. *Nat Commun.* 2020;11:3738.
57. Ke G, Meng Q, Finley T, Wang T, Chen W, Ma W, et al. LightGBM: A Highly Efficient Gradient Boosting Decision Tree. *Adv Neural Inf Process Syst* [Internet]. Curran Associates, Inc.; 2017 [cited 2023 Nov 19]. Available from: [https://papers.nips.cc/paper\\_files/paper/2017/hash/6449f44a102fde848669bdd9eb6b76fa-Abstract.html](https://papers.nips.cc/paper_files/paper/2017/hash/6449f44a102fde848669bdd9eb6b76fa-Abstract.html)
58. Perna A, Montine KS, White LR, Montine TJ, Cholerton BA. Paradigm shift: multiple potential pathways to neurodegenerative dementia. *Neurotherapeutics.* 2023;20:1641–52.
59. Thanaphong P, Link to external site this link will open in a new window, Brenna C, Link to external site this link will open in a new window, Mata IF, Link to external site this link will open in a new window, et al. Multivariate prediction of dementia in Parkinson's disease. *NPJ Park Dis* [Internet]. 2020 [cited 2021 Oct 25];6. Available from: <https://www.proquest.com/docview/2436973306/abstract/4285D58A0472424CPQ/1>
60. Li C, Ou R, Shang H. Rheumatoid arthritis decreases risk for Parkinson's disease: a Mendelian randomization study. *Npj Park Dis.* 2021;7:1–5.
61. Santiago JA, Potashkin JA. Shared dysregulated pathways lead to Parkinson's disease and diabetes. *Trends Mol Med.* 2013;19:176–86.
62. Paul R, Choudhury A, Borah A. Cholesterol – A putative endogenous contributor towards Parkinson's disease. *Neurochem Int.* 2015;90:125–33.
63. Ng Y-F, Ng E, Lim E-W, Prakash KM, Tan LCS, Tan E-K. Case-control study of hypertension and Parkinson's disease. *Npj Park Dis.* 2021;7:1–4.
64. Jozwiak N, Postuma RB, Montplaisir J, Latreille V, Panisset M, Chouinard S, et al. REM Sleep Behavior Disorder and Cognitive Impairment in Parkinson's Disease. *Sleep.* 2017;40:zsx101.
65. Sun A-P, Liu N, Zhang Y-S, Zhao H-Y, Liu X-L. The relationship between obstructive sleep apnea and Parkinson's disease: a systematic review and meta-analysis. *Neurol Sci.* 2020;41:1153–62.
66. Delic V, Beck KD, Pang KCH, Citron BA. Biological links between traumatic brain injury and Parkinson's disease. *Acta Neuropathol Commun.* 2020;8:45.
67. McCarter SJ, Stang C, Turcano P, Mielke MM, Ali F, Bower JH, et al. Higher vitamin B12 level at Parkinson's disease diagnosis is associated with lower risk of future dementia. *Parkinsonism Relat Disord.* 2020;73:19–22.
68. Beekly DL, Ramos EM, Lee WW, Deitrich WD, Jacka ME, Wu J, et al. The National Alzheimer's Coordinating Center (NACC) Database: The Uniform Data Set. *Alzheimer Dis Assoc Disord.* 2007;21:249.
69. Kannarkat GT, Boss JM, Tansey MG. The Role of Innate and Adaptive Immunity in Parkinson's Disease. *J Park Dis.* 2013;3:493–514.
70. Liu J, Zhang P, Zheng Z, Afridi MI, Zhang S, Wan Z, et al. GABAergic signaling between enteric neurons and intestinal smooth muscle promotes innate immunity and gut defense in *Caenorhabditis elegans*. *Immunity.* 2023;56:1515–1532.e9.
71. He D, Wu H, Xiang J, Ruan X, Peng P, Ruan Y, et al. Gut stem cell aging is driven by mTORC1 via a p38 MAPK-p53 pathway. *Nat Commun.* 2020;11:37.
72. Di Fusco D, Dinallo V, Monteleone I, Laudisi F, Marafini I, Franzè E, et al. Metformin inhibits inflammatory signals in the gut by controlling AMPK and p38 MAP kinase activation. *Clin Sci.* 2018;132:1155–68.
73. Li Z, Liang H, Hu Y, Lu L, Zheng C, Fan Y, et al. Gut bacterial profiles in Parkinson's disease: A systematic review. *CNS Neurosci Ther.* 2023;29:140–57.
74. Conway OJ, Carrasquillo MM, Wang X, Bredenberg JM, Reddy JS, Strickland SL, et al. AB13 and PLCG2 missense variants as risk factors for neurodegenerative diseases in Caucasians and African Americans. *Mol Neurodegener.* 2018;13:53.

## Publisher's Note

Springer Nature remains neutral with regard to jurisdictional claims in published maps and institutional affiliations.